2018

A REDUNDANT MONITORING SYSTEM FOR HUMAN WELDER OPERATION USING IMU AND VISION SENSORS

Rui Yu
University of Kentucky, rui.yu@uky.edu
Author ORCID Identifier:
https://orcid.org/0000-0002-6410-6088
Digital Object Identifier: https://doi.org/10.13023/etd.2018.465

STUDENT AGREEMENT:

I represent that my thesis or dissertation and abstract are my original work. Proper attribution has been given to all outside sources. I understand that I am solely responsible for obtaining any needed copyright permissions. I have obtained needed written permission statement(s) from the owner(s) of each third-party copyrighted matter to be included in my work, allowing electronic distribution (if such use is not permitted by the fair use doctrine) which will be submitted to UKnowledge as Additional File.

I hereby grant to The University of Kentucky and its agents the irrevocable, non-exclusive, and royalty-free license to archive and make accessible my work in whole or in part in all forms of media, now or hereafter known. I agree that the document mentioned above may be made available immediately for worldwide access unless an embargo applies.

I retain all other ownership rights to the copyright of my work. I also retain the right to use in future works (such as articles or books) all or part of my work. I understand that I am free to register the copyright to my work.

REVIEW, APPROVAL AND ACCEPTANCE

The document mentioned above has been reviewed and accepted by the student's advisor, on behalf of the advisory committee, and by the Director of Graduate Studies (DGS), on behalf of the program; we verify that this is the final, approved version of the student's thesis including all changes required by the advisory committee. The undersigned agree to abide by the statements above.

Rui Yu, Student

Dr. YuMing Zhang, Major Professor

Dr. Aaron Cramer, Director of Graduate Studies

A REDUNDANT MONITORING
SYSTEM FOR HUMAN WELDER OPERATION
USING IMU AND VISION SENSORS

THESIS

A thesis submitted in partial fulfillment of the
requirements for the degree of Master of Science in
Electrical Engineering in the College of Engineering
at the University of Kentucky

By

Rui Yu

Lexington, Kentucky

Director: Dr. YuMing Zhang, Professor of Electrical and computer Engineering

And Institute of Sustainable Manufacturing

Lexington, Kentucky

2018

ABSTRACT OF THESIS

A REDUNDANT MONITORING SYSTEM FOR HUMAN WELDER OPERATION USING IMU AND VISION SENSORS

In manual control, the welding gun's moving speed can significantly influence the welding results and critical welding operations usually require welders to concentrate consistently in order to react rapidly and accurately. However, human welders always have some habitual action which can have some subtle influence the welding process. It takes countless hours to train an experienced human welder. Using vision and IMU sensor will be able to set up a system and allow the worker got more accurate visual feedback like an experienced worker.

The problem is that monitor and measuring of the control process not always easy under a complex working environment like welding. In this thesis, a new method is developed that use two different methods to compensate each other to obtain accurate monitoring results. Vision sensor and IMU sensor both developed to obtain the accurate data from the control process in real-time but don't influence other. Although both vision and IMU sensor has their own limits, they also have their own advantage which can contribute to the measuring system.

KEYWORDS: Manual Welding Process. Vision Sensor, IMU Sensor, Recursive Least Square, Real-time Image Processing

Rui Yu
(Name of Student)

11/21/2018
Date

A REDUNDANT MONITORING
SYSTEM FOR HUMAN WELDER OPERATION
USING IMU AND VISION SENSORS

By

Rui Yu

YuMing Zhang

Director of Thesis

Aaron Cramer

Director of Graduate Studies

11/21/2018

Date

ACKNOWLEDGMENTS

The research work in this thesis is guidance by my advisor Dr. YuMing Zhang. I would like to sincerely thank him for his invaluable guide, continuous encouragement and constructive instructions. I am also want to thank all of my colleagues in the Welding Research Lab: Jinsong Chen, Chao li, YuTing Chen, WenHua Jiao for their helpful suggestions for my work.

In addition, I want to give my thanks for my parents for their endless support and love throughout all my lifetime.

TABLE OF CONTENTS

LIST OF FIGURES

CHAPTER 1. **INTRODUCTION**

1.1 Background

Monitoring and measuring of the control process are the core part for the factory to produce high-quality product. The difficulty of the control process sensing is how to collect accurate and precise information under some complex environment and motion state like GTAW welding show in Figure 1.1 [1], usually, the production process should be mechanized or automated as long as it can be justified for production cycle, cost, and quality. However, there is a lot of problems which adversely the automation significantly. Mechanized systems always require a very long time for on-site installation and prepared for great precision, furthermore, in some situation, there is not sufficient space for a huge automatic machine, also, a skilled worker can always have a better product quality than most of the machine. Therefore, the human-machine operation is still meaningful.

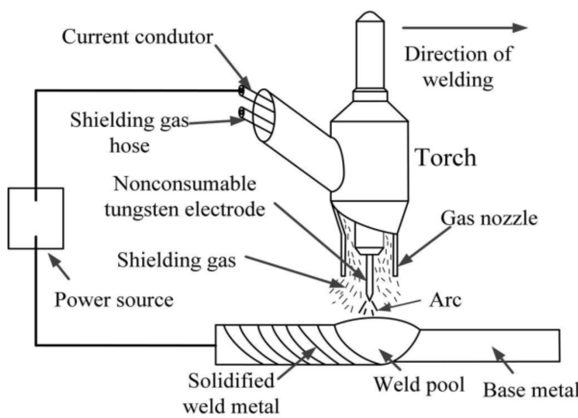

Figure 1.1: Illustration for GTAW welding

However, critical control operation requires works to concentrate consistently in order to react rapidly and accurately. Like in the welding process, fatigue and stress build up quickly so that welders' capabilities degrade rapidly. We always want to assure the product quality. It brings us to the mechanized welding, however, welder can't interfere with the system in mechanized welding. Robotic also can't observe the welding process with the same level of concentration as in manual operation. Mechanized systems rely on precision control of joint fit-up and welding conditions and tedious programming to produce repeatable results, but it's obvious that precision control of joints and welding conditions is very costly and not always guaranteed. Up to date, there are no sensor/ways that can be conveniently carried by the torch automatically monitor the penetration depth or the degree of full penetration like a skilled worker.

There has a major difference between machine and human in the production cycle. It takes countless hours to train a proficient human worker to make sure that he/she has the ability to acquire accurate and enough quality-related information using his/her sophisticated sensing system to finish the work. For the automatic applications, repetitive and uncomplicated work has already been replaced by the machine in the manufacturing industry ([2],[3],[4]), since, a well-designed system has excellent stability and physical properties beyond the human body.

For the control process, using the automatic machine or human workers depends on the different needs. the implementation of an automatic control requires worker understood mechanistic approaches and control algorithms. The ability of a skilled worker to control the producing process is not due to a fundamental understating of the laws of physics but based on the feedback sensory information which might be imprecise or partial truths.

1.2 Objective and approach

Robotic and manual workers both have their own advantages and limits. A human worker has many different experiences and can easily adjust for different circumstances, but, they have their physical limitation which makes human worker can’t operator some of the heavy machines. Robotics is suitable for precision and repeated massive production applications but need a long time and high cost to set up. In other words, a very long preparing time and not suitable for a small amount of application. The objective here is to design an appropriate system to detect and provide more accurate data to help improve the performance of human works control process. Specifically, the tasks of this study are

1. To take advantage of the human worker’s natural movement to facilitate automatic process monitoring.
2. Provide more accurate and reliable information to human work help them adjust their control process.
3. Provide a method using two different sensor’s to compensate each other to obtain accurate monitoring results.

1.3 Organization

In this thesis, a cooperative sensing system is developed to provide accurate and reliable data to assist a human worker to judge how to adjust the current process situation.

Chapter 1: Introduction

The background and motivation of this dissertation are illustrated, and the objective of this study is also introduced. Discussed the related technologies in this field and have some think about future developments.

Chapter 2: Literature review

Introduced the related technologies in this field and have some discussion about future developments in the related technologies.

Chapter 3 Image processing

In this part, the camera techniques and computer vision technology are introduced about image denoise, analysis. After calibration, it can roughly be divided into three steps as segmentation, classification and tracking. With the feature detected from the processed image, it will be able to track the information that control process needed.

Chapter 4 Inertial measurement unit sensing system

The IMU sensors model has been set up, after calibration, we use recursive least square method to process the data and update the prediction model when the error surpass a specific value.

Chapter 5 Conclusion and Future work

Summarize the work which have already been finished and the future research work to improve this study is also introduced.

CHAPTER 2. **LITERATURE REVIEW**

2.1 Overview

Although automatic control process has been widely applied in manufacturing industries like aircraft production, automotive assembly or micro-electric components joining. It's highly likely that intelligent and accurate automatic system is becoming the next trend for the factory production. There's still a lot of challenge in the automatic fields like how to monitor and control the production process accurate, reliably and cost-effectively. Therefore, there's still has various techniques underdeveloped for manual process.

2.2 Computer Graphic

Computer graphic has been widely applied in manufacturing industries and real life, such as automotive assembly, human presence detection or autonomous driving. Intelligent and accurate segmentation and classification is the trend for the next generation. The major challenge in both industry and real life is to make it fast, reliable safety and cost-effectively.

Computer graphic has some typical tasks like recognition, motion analysis, scene reconstruction or image restoration. Usually, the approach was pretty same, from start to the end, it will be image acquisition, pre-processing, feature extraction, detection/segmentation, high-level processing and decision making. Due to the hardware's fast evolution include range sensor, tomography devices, radar, ultra-sonic cameras, etc. Today's most computer vision system has better performed than human and highly stable. There are three major categories in the computer graphic fields. First, image processing, doing some transform on the input image, output usually still was an image, which basically does not involve or rarely involves analysis of the image content. Typical examples were image enhancement, image denoising [18] or binary image processing, etc. segmentation based on threshold also falls within the scope of image processing. Generally dealing with a single image. Second, image analysis, analysis of the content of the image and extract meaningful features for subsequent processing. Still only process a single image. Third, computer vision, analysis the features obtained from image analysis, extract the semantic representation of the scene, process a sequence image.

Image process is actually digital image processing, is to project the real three-dimensional random signal in the real word to the two-dimensional plane of the sensor, sampled and quantized to obtain a two-dimensional matrix. Digital image process is to recover the three-dimensional scene from the 2-D matrix. This involves three important attributes about an image is continuity, two-dimensional and randomness.

Signal processing and pattern recognition, especially pattern recognition, was one of the most successful methods in the past ten years, typical like Boosting [5], Clustering [6], Compressive Sensing [7] or Decision tree [8], are all widely used in the computer vision fields. Therefore, it will be able to apply a vision-based system to act as human worker's eyes, i.e., to acquire the image of the complete control and manufacturing process, with the information extract from the image, the related control algorithms will be applied to adjust the process for some specific quality requirement.

2.3 IMU Sensor Technique

Motion detect sensors are inertial measurement units (IMU), and it was widely used in specific fields like navigation and mapping tasks.

With the help from the gyroscope, IMU sensor [9] can give us some real-time reaction with the acceptable error's data which could be used to estimation the orientation of the torch. With some real-time's filter's (like unscented Kalman filter or Recursive least square estimation) help. The result was highly accurate and immediate, but there are still some problem's like errors accumulation, also, most of the filter only works well for the high-speed movement like car or unmanned aerial vehicle, when the situation changes to some very slow and precise environment, the instrument error carried from the IMU sensor itself like temperature, gyro's constant drift or degree's random drift will be obviously enlargement. And because those errors were came with instruments measurement, it is inevitable that the calculation will contain errors we need to consider.

In pure visual SLAM or VO [9]. Due to the motion blur, occlusion, fast motion, pure rotation, and scale uncertainty of the image, it is difficult to complete the application requirements of an actual scene with only one camera, In order to monitoring and measuring the control process with acceptable error, an IMU sensor can directly obtain the measurement data of the angular velocity and acceleration of the moving subject, thereby, it can constrain the object's motion or complement the visual system, it can realizing the positioning of the fast motion or pure rotation's process to further improving the reliability of SLAM/VO. IMU's data frequency is generally much higher than visual, in two visual frames, k, k + 1, it will usually have more IMU data, like angular data, quaternion expression and instant velocity. Although those data had constant errors, there still some research [10] try to reach a more accurate result with multiple inertial measurement units with data fusion algorithms.

But the problem is still that in some specific process like GTAW process, how to use an IMU sensor measure the accurate control result in a relatively slow and smooth moving process is still hard, the acceleration generated from the human control is relatively small compared to the acceleration from the gravity, it’s hard to use accelerometer in this kind of control process.

CHAPTER 3. **IMAGE PROCESSING**

3.1 Calibration

The calibration in this paper is in addition to the WeiJie Zhang and HongSheng's paper [1]. Including the chapter and the appendix.

In the image measurement process and machine vision application, in order to determine the relationship between the three-dimensional geometric position of a point on the surface of the space object and it's corresponding point in the image, a geometric model if the camera imaging must be established. this geometric model's parameters are camera parameters, under most conditions, these parameters must be obtained through experiments and calculations. Whether in image measurement or machine vision application, the calibration of camera parameters is a very critical part. The accuracy of the calibration results and the stability of the algorithm directly affect the accuracy of the results produced by the camera.

An appropriate system calibration is necessary for the accurate image in the study. In the experiment set-up, there are mainly two categories of system errors.

1. Set-up errors for the camera and the target object, which might lead to static errors for the data collection.
2. Camera distortion may cause the deformation of the captured image.

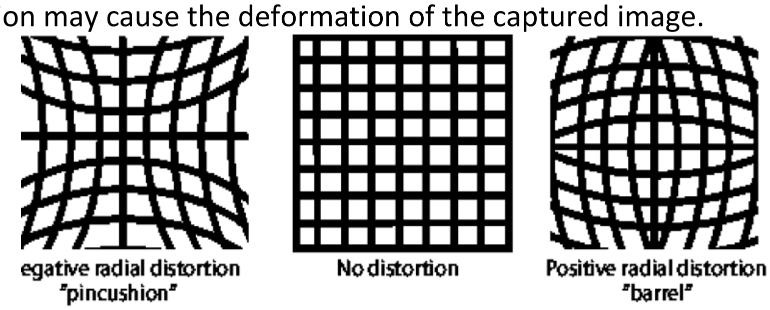

Figure 3.1: The deformation of the camera

The camera internal model in [11] is adopted which includes the following internal parameters:

1. Focal length vector f_c: The focal length in pixels of the camera.
2. Principal point vector c_c: The principal point coordinate in the camera frame.
3. Skew coefficient α_c: The skew coefficient defining the angle between the x and y pixel axes.
4. Distortions vector k_c: The image radial and tangential coefficients ([12],[13]).

The focal length, principal point and the skew coefficient consist of the intrinsic matrix of the camera are show in Equation. 3.1.

$$H = \begin{bmatrix} f_{cx} & \alpha_c * k_{cx} & c_{cx} \\ 0 & f_{cy} & c_{cy} \\ 0 & 0 & 1 \end{bmatrix} \tag{3.1}$$

Where $f_c = [f_{cx} \quad , \quad f_{cy}]$ and $c_c = [c_{cx} \quad , \quad c_{cy}]$.

The target of calibration is to target the camera on a known structure, usually use a chessboard, because it has many individual and identifiable grid. By viewing this structure from a variety of angles, it will be able to compute the relative location and orientation of the camera at the time of each image and the internal parameter of the camera [14]. In this study, the chessboard is making by a chessboard paper attached on the image plane, as shown in Figure 3.2. In the first image, the camera is not in the horizontal line of the chessboard. The second and third image was the image with the perspective transformation with matrix H_P, finial, we can establish a coordinate system.

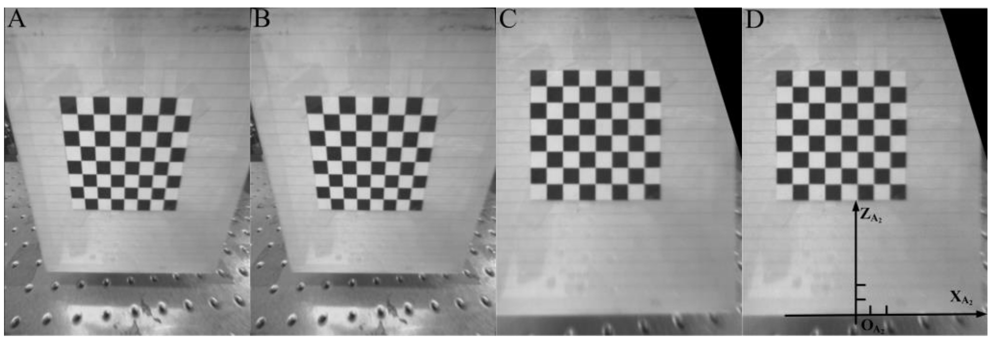

Figure 3.2: Results of camera and imaging plane calibration: A) The original image of the chessboard; B) Result of camera distortion correction; C) Result of frontal parallel view for the chessboard; and D) The conversion to the $(oxyz)_{A2}$ coordinate system

Using the calibration process in ([15],[16]), radial and tangential distortion are obtained from Figure 3.3: How the radial and the tangential distortion of the camera influence the image And the H will be are show in Equation. 3.2.

$$H = \begin{bmatrix} 297.5 & 0 & 250.5 \\ 0 & 297.5 & 341.4 \\ 0 & 0 & 1 \end{bmatrix} \tag{3.2}$$

The distortions vector k_c are shown in Equation. 3.3.

$$k_c = [-0.0077 \quad -0.0053 \quad 0.0002 \quad 0.0011 \quad 0.0061] \tag{3.3}$$

The position and the orientation of the chessboard in the image can be calculate. Therefore, a perspective transformation matrix H_P can be obtained in the Equation. 3.4.

$$H_P = \begin{bmatrix} 31.64 & 8.27 & 142.18 \\ 0.31 & 41.53 & 207.89 \\ -0.0004 & 0.038 & 26 \end{bmatrix} \tag{3.4}$$

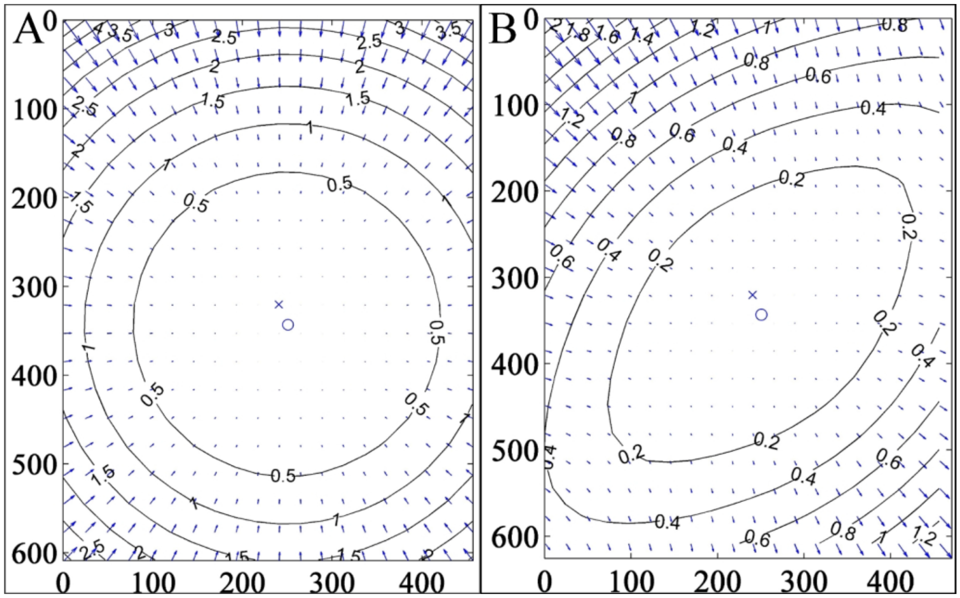

Figure 3.3: How the radial and the tangential distortion of the camera influence the image

3.2 Denoise

Basically, every image from the camera has a lot of feature data, it will relatively hard to extract our interesting area from an original image cause the noise.

Gaussian blur [17] is a data smoothing technology and widely used in the image processing field. It’s a Low-pass filter which means it can reduce image noise and reduce image detail. Roughly speaking, gaussian blur can be understand as each pixel takes the average value of the surrounding pixels. However, Images are always continuous, which means that closer points obviously have more influence than the long distances points. Therefore, the weighted average is more reasonable than the normal average.

We will use normal distribution here.

$$f(x) = \frac{1}{\sigma\sqrt{2\pi}} e^{-(x-\mu)^2/2\sigma^2} \tag{3.5}$$

$$f(x) = \frac{1}{\sigma\sqrt{2\pi}} e^{-x^2/2\sigma^2} \tag{3.6}$$

$$G(x,y) = \frac{1}{2\pi\sigma^2} e^{-(x^2+y^2)/2\sigma^2} \tag{3.7}$$

In Equation. 3.1, μ is the mean of x, σ is the variance of x. Because the centre point is the origin point when calculating the average, therefore, μ can be considered as zero, which leads us to the Equation. 3.2. According to the one-dimensional Gaussian function, a two-dimensional function can be derived as Equation.3.3. The weight of every point can be calculated using the two-dimensional function Equation. 3.3.

14	15	16	14x0.0947416	15x0.118318	16x0.0947416
24	25	26	24x0.118318	25x0.147761	26x0.118318
34	35	36	34x0.0947416	35x0.118318	36x0.0947416

Figure 3.4: Weight matrix of Gaussian blur

For the edge part [18], Although the edge part only has half matrix make it impossible to compute the normal weight matrix. It still has an alternative way, by copy the matrix from the corresponding positions on the other side, it will be able to reconstruct a complete matrix for the weight matrix.

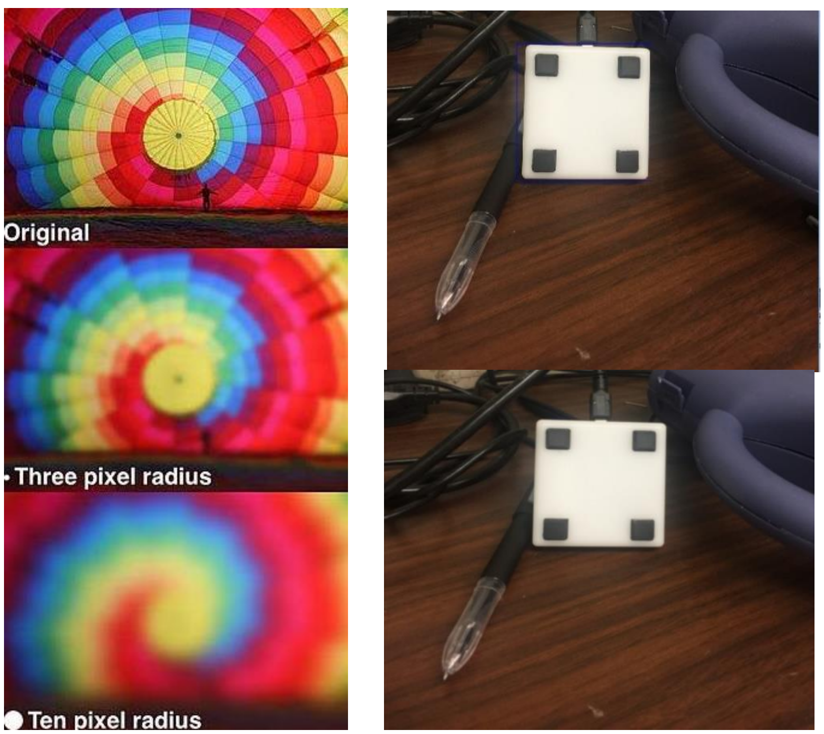

Figure 3.5: Gaussian blur

After the gaussian blur, the image needed to transform to grayscale in order to calculate the gradient of the image. The grayscale of the image can be considered as the image's intensity, the direction of the gradient is the fastest change in the image's function $G(x, y)$. When there is an edge in the image, there must be a large gradient value, we can get the gradient image through computing the gradient of each pixel in the image. Which shows in the Equation. 3.4, 3.5, 3.6.

$$G(x, y) = dx(i, j) + dy(i, j) \tag{3.8}$$

$$dx(i, j) = l(i + 1, j) - l(i, j) \tag{3.9}$$

$$dy(i, j) = l(i, j + 1) - l(i, j) \tag{3.10}$$

L was the image's grayscale value and I, j is the pixel's coordinate.

The edge of the image contains a lot of gradient information, edge detection based on the gradient is simple and effective. However, in order to obtain a more accurate positioning of the boundary, it is necessary to consider the influence of non-edge points with large noise and gradient. In this case, the image information needs more complicatedly process.

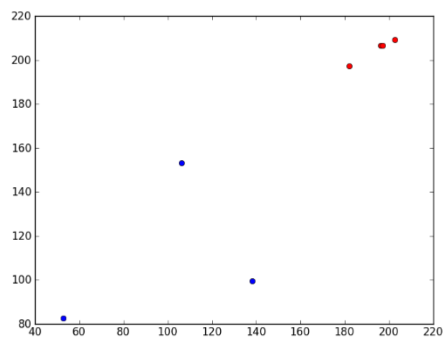

Figure 3.6: The grayscale's median distribution

This Figure 3.6: The grayscale's median distribution shows that the interesting objects grayscale's level was concentrate on the right-top corner.

3.3 Segmentation

In order to extract the interesting area from the background in the image, an appropriate segmentation is required which can be determined by analyzing the histogram of the image, as shown in Figure 3.7, It can be observed that most pixels are concentrated in specific levels, Most of those pixels can be considered as the background and possibly part of the noise, therefore, the threshold for a binary segmentation will be able to decided.

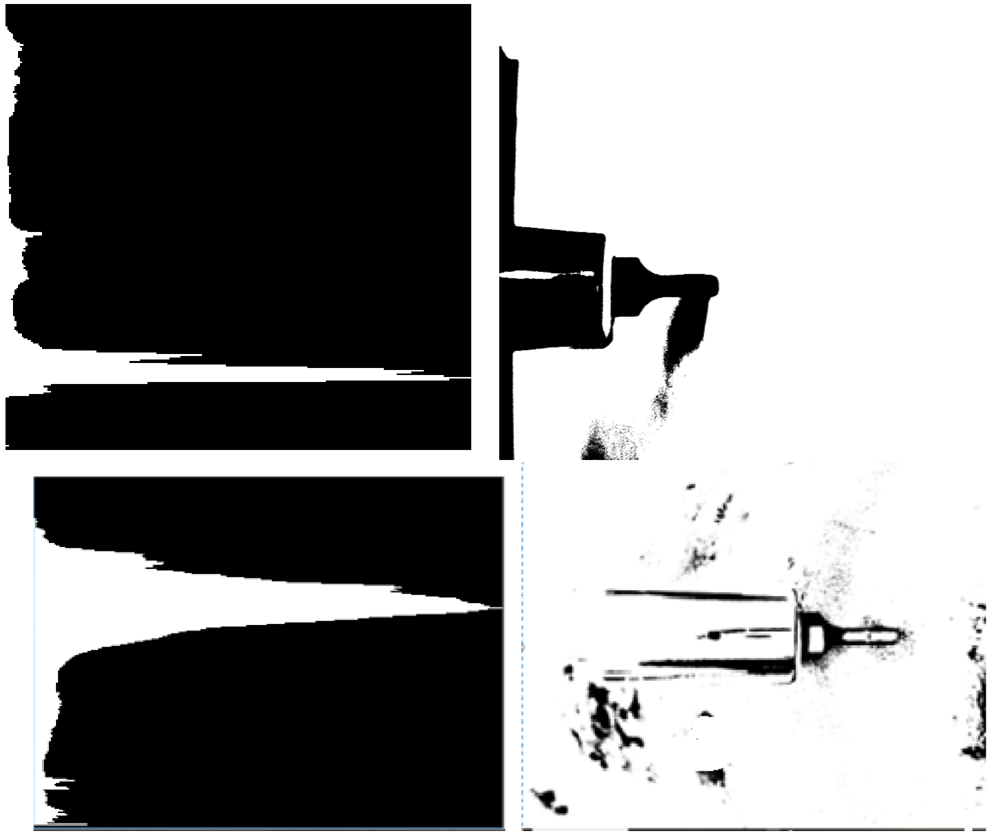

Figure 3.7: Histogram image and threshold image

This kind of binary can effectively identify most of the area we are interested in. However, it still has some noise in the image since the binary segmentation is not an adaptive thresholding algorithm, it can lose uncertain numbers of features we want and keep some fake data we don't need. Those problems we are solved in the next part, Morphology process.

Morphological image processing like dilation, or erosion, is a collection of non-linear operations related to the shape or morphology of features in an image, it uses a small shape or template called a structuring element doing the opening or closing operation. They are both derived from the fundamental operations of erosion and dilation and usually only applied to the binary image. The opening operation will eliminate small clumps of undesirable foreground pixels and closing operation will fill small background colour holes in the image. Therefore, those operations can significantly remove the image's Irregular edge noise.

Opening operation, in fact it is the processing of eroding first and then dilating, if dilating first and then eroding, it will be called as closing operation, showing in Equation 3.7, 3.8.

$$dst = close(src, element) = erode(dilate(src, element)) \tag{3.11}$$

$$dst = open(src, element) = dilate(erode(src, element)) \tag{3.12}$$

The closing and opening operation are shows in Figure 3.8.

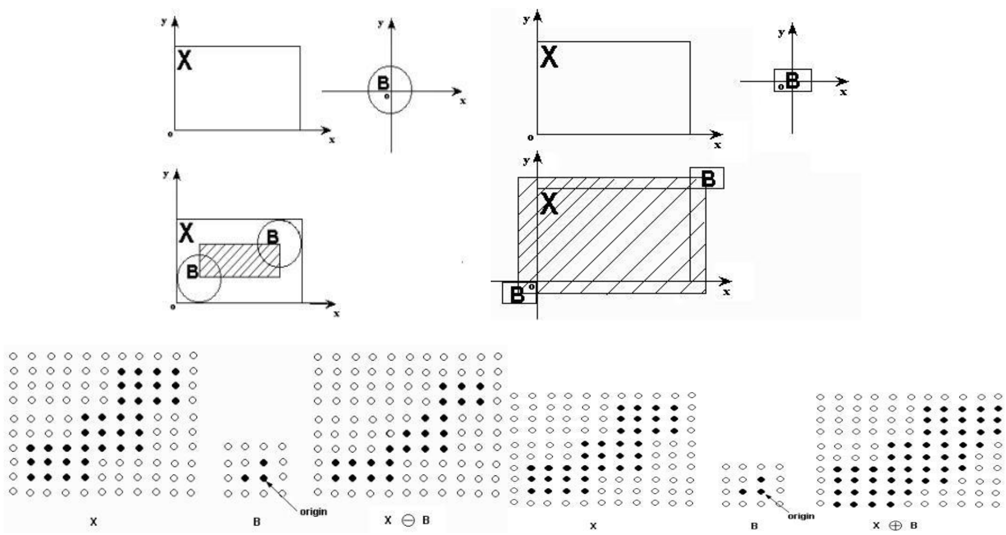

Figure 3.8: Opening and closing operation

With the appropriate structure element, we can obtain the image in Figure 3.9. Use the oval element first to erase the noise and the object's connection. Then change to the cross element to mark the object area. We can see that the black noise connected with the object has been removed after the morphological process.

Figure 3.9: Morphology process with different struct element

Obviously, we will lose some part of the image in this way and the lost part might not able to be retrieved, but to the end, it will not influence the result cause the only data we interested here is the motion state of the entire object. By calculating the centroid in shown in Figure 3.10, the influence will not be count.

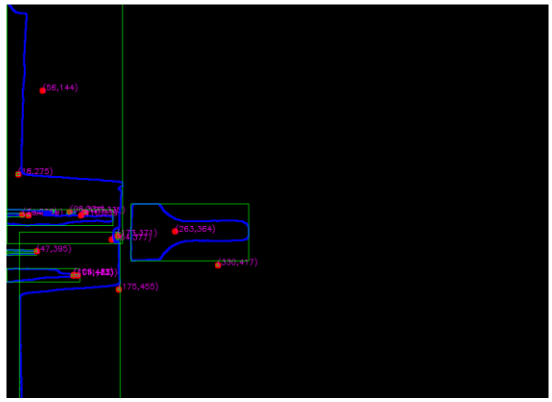

Figure 3.10: Centroid of the objective

3.4 Tracking

With the image after all process, it will be an image without too many interferences, it's will be relatively easy to track the feature from the image that we needed during experiment, with an auxiliary line swing from 0 degrees to 360 degrees. Every time the line crossing the object's, we will count it. In the end, it will give us a sequence of data shows in Figure 3.11. It's obvious that there has a unique degree which the line cross the object's lowest times.

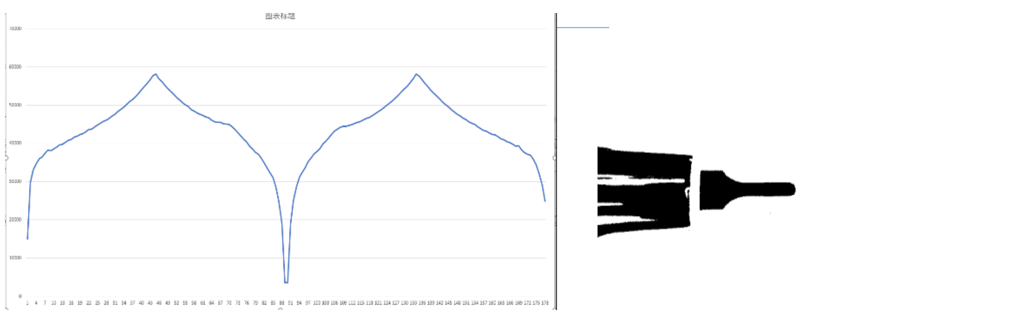

Figure 3.11: relative degree of the torch and count and the degree of the torch

The unique degree shows that we can extract a feature from the image which related to the object's degree. The relative relationship of the auxiliary line's degree and the object's degree can provide us with the information that we needed to calculate the object's degree in real time

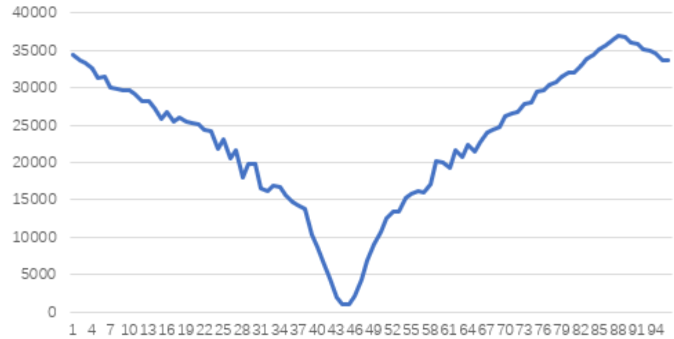

Figure 3.12: Degree of the torch

The results show that in the most part of the rotation process, the torch's motion could be analyzed by the vision sensor but when it goes to a specific orientation, the vision sensor will lose the object's characteristics features and lose the accurate degree. In the next inertial measurements unit sensor part, we tried to obtain another patch of data from a different system which has the potential to help improve the final monitoring results.

CHAPTER 4. **INERTIAL MEASUREMENT UNIT SENSING SYSTEM**

4.1 Introduction and related works

The measurement of the object's movement motion, using the proposed IMU sensing system requires to detect the object's orientation in real-time. In this section, the orientation of the projective object, as an example, is estimated using a recursive least square-based algorithm.

The objectives orientation is defined as the object's posture throughout an experiment process. It is one of the most important features for a control system. Optimal quality result can only be guaranteed if the object's orientation is accurate adjusted. Inappropriate control process can cause various problems ([19],[20]) on the result. Therefore, some accurate data about the object's orientation was required.

Mastering the object manipulation is challenging for a human worker to manually control the object with a specific posture and move smoothly under the limited of the human body. It is usually highly depending on the worker's skill level and his/her physiological conditions [21]. Which means, the corresponding measurement scheme should be robust enough to make sure the measurement accuracy was able to against the disturbances caused by the worker's operations and this was the basic goal of the chapter for.

This chapter aims to develop an appropriate method to measure the accurate 3-D orientation of the torch which could be able to use in real manual welding process or welding training system. Based on a little change about the Recursive least square algorithm, we hope to reduce the noise from the sensor and can estimate the torch's motion in real time. In addition, a quaternion was used to represent the angular position since it can reduce the time complexity and avoid gimble lock problem which Euler angles system have [22].

4.2 Representation of object's orientation

As shown in Figure 4.1 [1]. The IMU sensor is mounted rigidly at the tail of the torch using a plastic fixture. The 3-D coordinate frame. Express as ${}^{s}(xyz)$, is the IMU sensor's internal frame. It doesn't need to be considered too much because, during the assembly process, the torch was first held still let the handle perpendicular to the gravitation direction, with the help from the external calibration tools, such as gravimeter, we can make sure that the gravitational acceleration only needs to be considered as ${}^{s}Z$ axis.

The coordinate frame ${}^{t}(xyz)$ is the internal frame for the object's, axis ${}^{t}Z$ is coincides with the object's head direction, ${}^{t}X$ coincides with ${}^{s}X$. It means that rotate the frame ${}^{s}(xyz)$ with a specific angle will obtain ${}^{t}(xyz)$, the angle was θ_{st}.

The object's orientation is determined when the axis orientation of the coordinate frame ${}^{t}(xyz)$ is obtained from an absolute 3-D Cartesian coordinate frame and expressed as ${}^{E}(xyz)$. The negative direction is a coincidence with the local gravitational direction and defined as ${}^{E}Z$. Depends on the different process, the other two axes direction may change.

The tri-axial gyroscope in the IMU sensor measures the angular velocity of the frame ${}^{s}(xyz)$ relative to frame ${}^{E}(xyz)$. The measurement (in rad/s) can be denoted by a 1-by-3 row vector shown in Equation. 4.1.

$$ {}^{s}\omega = [\omega_x,\ \omega_y, \omega_z] \tag{4.1} $$

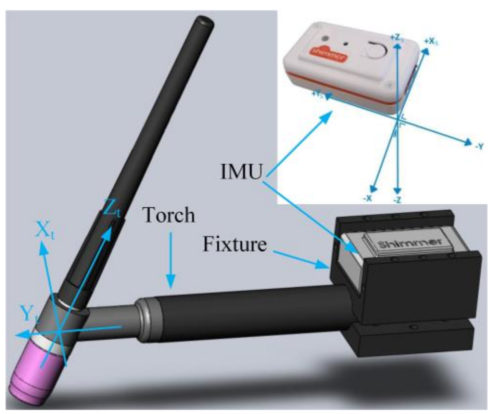

Figure 4.1: The illustration of troch and IMU system, ${}^{s}(xyz)$ and ${}^{t}(xyz)$ denote the 3-D coordinate system for the torch and the WIMU, respectively.

The object's orientation is denoted by a quaternion list below as Equation. 4.2. Where x, y, z express three different axes and ω express angle. Norm list as Equation. 4.3.

$$ |q| = \sqrt{x^2 + y^2 + z^2 + \omega^2} \tag{4.2} $$

$$ \|q\| = x^2 + y^2 + z^2 + \omega^2 \tag{4.3} $$

The quaternion and k instant can be derived from $k-1$ instant with angular measurement $({}^{s}\omega_k)$ and time interval denoted by T_s [5].

$$ {}_{E}^{s}\tilde{q}_{k+1} = {}_{E}^{s}\tilde{q}_{k} \otimes \exp\left(\frac{T_s}{2}\omega_k\right) \tag{4.4} $$

Where $\otimes$ is the quaternion product, which is defined in Equation. 4.5. $\exp(.)$ defined in Equation. 4.7.

$$q_1 \otimes q_2 = (s_1 \cdot s_2 - v_1 \cdot v_2, s_1 \cdot v_2 + s_2 \cdot v_1 + v_1 * v_2) \tag{4.5}$$

Because $q = \omega + xi + yj + zk$ can be divided as scalar ω and vector $xi + yj + zk$. It can be express as $\mathrm{q} = (\mathrm{s}, \mathrm{v})$ where s is scalar ω and v is vector $xi + yj + zk$, so, the product can also be denoted as Equation. 4.6.

$$q_1 \otimes q_2 = \begin{matrix} (\omega_1\omega_2 - x_1x_2 - y_1y_2 - z_1z_2) + \\ (\omega_1x_2 + x_1\omega_2 + y_1z_2 - z_1y_2)i + \\ (\omega_1y_2 - x_1z_2 + y_1\omega_2 + z_1x_2)j + \\ (\omega_1z_2 + x_1y_2 - y_1x_2 + z_1\omega_2)k \end{matrix} \tag{4.6}$$

$$exp(v) \triangleq \left[\cos(|v|), \frac{v}{|v|}\sin(|v|)\right] \tag{4.7}$$

Where v presents 1-by-3 row vector. With all the Equation above, the object's orientation will not be able to calculate and express through an accurate coordinate system.

4.3 Sensor Modeling

The inertial measurement unit system based on the gyroscopes and accelerometers to measure the object's specific force, angular rate and sometimes the magnetic fields, not always can measure magnetic fields because some of the IMU sensors don't have magnetometer in it. Limits here is that the IMU sensor' suffers a lot of errors like zero drift or scale factor problem, etc. Figure 4.2 shows that the data from the sensor has errors even the object didn't move. This kind of error called zero drift or other errors like error accumulation or voltage fluctuations shown in Figure 4.3. Although it was a constant deviation and can be compensated by subtracting an average value from the output, it will still influence the result. The other problem is that the acceleration generated in smooth control process like manual welding is relatively small when compared to the gravity acceleration, which means that it's hard to use the accelerometer in the IMU sensor in this kind of control process.

Those errors are common in the instrument used to calculate position or velocity. Because those errors are in the instrument's measurements, it is inevitable that the calculations will contain errors. In the next part, the error source will be analysis and the mathematic model will be used to deal with the errors.

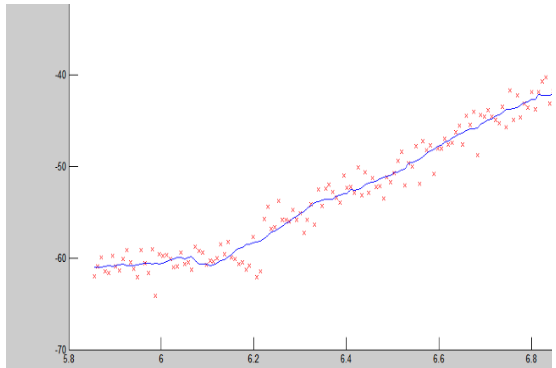

Figure 4.2: The original output from the IMU sensor

The gyroscope and the accelerometer in the IMU sensor measure the angular velocity and the acceleration of the sensor respectively. Other than the true values, $s_{\omega_{true}}$ and $s_{a_{true}}$, there are several specific errors may affect the measurements of the IMU sensor, like measurement noise, bias, scale-factor instability. Therefore, the IMU sensor's data and itself still needs some dispose. The $s_{\omega_{true}}$ and $s_{a_{true}}$ are shown in Equation. 4.8. and Equation.4.9.

$$^{s}\omega = S_{\ \omega} s\omega_{true} + b_{\omega} + v_{\omega} \tag{4.8}$$

$$^{s}a = S_{\ a} sa_{true} + b_{a} + v_{a} \tag{4.9}$$

In the equation, s_{ω} and s_{a} are the scale-factor matrices, b_{ω} and b_{a} are the bias, v_{ω} and the v_{a} are the measurement noises. Cause this is just a simplified sensor model. Some minor error sources will not be considered, such as gravity-sensitivity or cross-sensitivity.

Usually, the measurement noises v_{ω} and the v_{a} can be considered as white Gaussian noise, with a covariance matrix and a null mean respectively. The covariance matrix of the sensor model list as Equation 4.10.

$$\mathrm{R} = \begin{bmatrix} R_{\sigma_{\omega}^{2}} I_{3x_{3}} & 0 \\ 0 & R_{\sigma_{a}^{2}} I_{3x_{3}} \end{bmatrix} \tag{4.10}$$

The two components which influence the true acceleration measurements was the sensor acceleration and the gravitation acceleration, as expressed by Equation. 4.11.

$$^{s}a_{true} = \ ^{s}a_{sensor} + \ ^{s}g \tag{4.11}$$

In here, ^{s}g is the gravitational acceleration in the sensor frame. The object should be moved smoothly during the experiment. Thereby, $^{s}a_{sensor}$ is relatively small compared to the gravitation acceleration. Henceforth, Equation 4.11 can be expressed as Equation. 4.12.

$$^{s}\tilde{a}_{true} \cong {}^{s}\tilde{g} \tag{4.12}$$

By using normalized gravity can eliminate the measurement error caused by localized gravity difference.

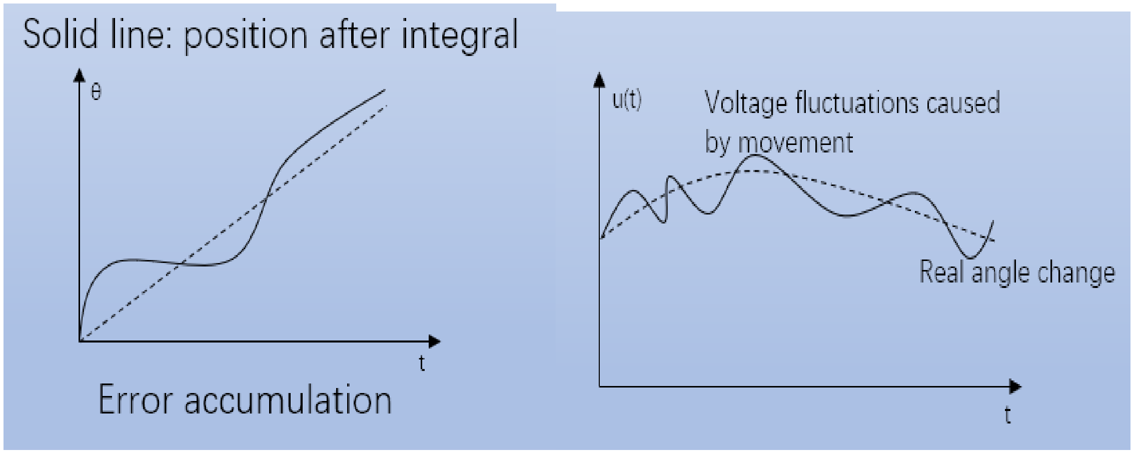

Figure 4.3: IMU sensor's error accumulation and Voltage fluctuation

The scale and the bias factors, in Equation 4.8. and Equation 4.9. depending on the sensors' imperfections and the working field. The typical gyro bias is 0.017-0.17 rad/h and acceleration bias is about 100-1000 μg for tactical grade [23]. Also, the ambient temperature significantly affects the gyro's bias. Hence, sometimes when the IMU sensor was put near a strong heat source, the gyro's bias will not be constant throughout the measurement. That's why a camera system could be able to help compensate the gyro's drift in-line to guard the effect of the drift variation over temperature to the estimation accuracy.

Although the influence of temperature on the accelerometer's bias is much less intense. The in-line calibration of an accelerometer always requires the accelerometer remaining in a static condition for several different orientations [24]. But in this application, the objective was assumed to hold for a certain orientation. Therefore, the accelerometer bias can be assumed as constant and will be compensated by the calibration before use [25].

The scale factor drifts of IMU are known to affect the measurement accuracy to a much less extent than the bias drifts, also, drift variation over temperature area same negligible [26]. Therefore, the scale factors were only relatively small variations around their average values throughout the experiment process. Their nominal value will be determined through the sensor calibration before using [25].

For the calibration part. Because the system error caused by the shacking or many other resources will change the sensor's internal parameter, which means that the IMU sensor needs to calibration precisely every time before ready use. Which means we need to use current information to establish a new relation system for the sensor. Accuracy error of the gyro sensors which might result in the position or orientation measurement errors and then leads to unpredictable results. The IMU sensor used in this process provides a well-developed software to do the calibration process, so, we will not discuss the calibration process here.

4.4 System Analysis

Adaptive filter belongs to the category of modern filtering. It is an important application in the field of adaptive signal processing developed in the 1940s. Adaptive signal processing is mainly to study a system with variable or adjustable structure, which can be in contact with the outside world in order to improve the performance of signal processing, usually, such systems are always time-varying nonlinear systems that can automatically adapt to the environment and requirements of signal transmission without having to know the structure and actual knowledge of the signal in detail.

The least squares method is a standard approach in regression analysis to approximate the solution of overdetermined systems. The original principle of least squares was first carried out by mathematicians such as C. F. Gauss, A. M. Legendre and R. Adrain. and the Recursive least squares was an adaptive filter algorithm that recursively finds the coefficients that minimize a weighted liner squares cost function relating to the input signals, in other words, the current solution can be calculated by update the previously processed solution (using old observation data) with new observations. The error function is defined as Equation. 4.13.

$$e(i) = d(i) - y(i) = d(i) - W^H(n)U(i) \quad (4.13)$$

In here, $d(n)$ is expected response, $U(i)$ is input vector, $W^H(n)$ is filter update with time.

The recursive least squares cost function is defined as follows

$$\varepsilon(n) = \sum_{i=1}^{n} \beta(n,i)\left|e(i)\right|^2 + \sigma\lambda^n \left\|W(n)\right\| \quad (4.14$$

The λ here is forgotten factor, the introducing of the forgotten factor make the RLS algorithm able to track non-stationary signals. Roughly speaking, the reciprocal of $1-\lambda$ can be used to describe the memory ability of the algorithm.

The input vector $U(i)$'s relation with average time matrix and with expected response vector can be express as Equation 4.15. Equation 4.16.

$$\Phi(n)=\sum_{i=1}^{n}\lambda^{n-i}U(i)U^{H}(i)+\sigma\lambda^{n}I \tag{4.15}$$

$$Z(n)=\sum_{i=1}^{n}\lambda^{n-i}U(i)d^{*}(i) \tag{4.16}$$

Therefore, the regular equation of the recursive least squares can be written as Equation 4.17. And can derive to Equation 4.18. from Equation 4.15.

$$\Phi(n)\hat{W}(n)=Z(n) \tag{4.17}$$

$$\Phi(n)=\lambda\left[\sum_{i=1}^{n}\lambda^{n-1-i}U(i)U^{H}(i)+\sigma\lambda^{n-1}I\right]+U(n)U^{H}(n) \tag{4.18}$$

The equation in the square brackets can be expressed as $\Phi(n-1)$, therefore. Use the same theory. We will have Equation 4.19. Equation 4.20.

$$\Phi(n)=\lambda\Phi(n-1)+U(n)U^{H}(n) \tag{4.19}$$

$$Z(n)=\lambda Z(n-1)+U(n)d^{*}(n) \tag{4.20}$$

The $\Phi(n-1)$ in here express the previous observation data, and the $U(n)U^{H}(n)$ acting as the correcting factor during the update process. With the help from the Matrix inversion lemma, if A and B are two $M\times M$ Positive moment and C and D are $M\times N$, $N\times M$ matrix, have relation in Equation 4.21. Equation 4.22.

$$\mathrm{A}=\mathrm{B}^{-1}+\mathrm{C}\mathrm{D}^{-1}\mathrm{C}^{\mathrm{H}} \tag{4.21}$$

$$\mathrm{A}^{-1}=\mathrm{B}-\mathrm{BC}(\mathrm{D}+\mathrm{C}^{\mathrm{H}}\mathrm{BC})^{-1}\mathrm{C}^{\mathrm{H}}\mathrm{B} \tag{4.22}$$

Assume we have relation in Equation 4.23.

$$\begin{aligned}\mathrm{A}&=\Phi(n)\\ \mathrm{B}^{-1}&=\lambda\Phi(n-1)\\ \mathrm{C}&=U(\mathrm{n})\\ \mathrm{D}&=1\end{aligned} \tag{4.23}$$

We will obtain Equation 4.24.

$$\Phi^{-1}(n)=\lambda^{-1}\Phi^{-1}(n-1)-\frac{\lambda^{-2}\Phi^{-1}(n-1)U(n)U^{H}(n)\Phi^{-1}(n-1)}{1+\lambda^{-1}U^{H}(n)\Phi^{-1}(n-1)U(n)} \tag{4.24}$$

In here, we let $P(n)=\Phi^{-1}(n)$ and $K(n)=\dfrac{\lambda^{-1}P(n-1)U(n)}{1+\lambda^{-1}U^{H}P(n-1)U(n)}$, will derived Equation 4.25.

$$P(n) = \lambda^{-1} P(n-1) - \lambda^{-1} K(n) U^H(n) P(n-1) \quad (4.25)$$

$M \times M$ matrix $P(n)$ was Inverse correlation matrix, $M \times 1$ vector $K(n)$ was gain vector. Simplify the $K(n) = \dfrac{\lambda^{-1} P(n-1) U(n)}{1 + \lambda^{-1} U^H P(n-1) U(n)}$, we can obtain the Equation 4.26.

$$K(n) = \lambda^{-1} P(n-1) U(n) - \lambda^{-1} K(n) U^H(n) P(n-1) U(n) \quad (4.26)$$

Therefore, same as Equation 4.27.

$$K(n) = \left[\lambda^{-1} P(n-1) - \lambda^{-1} K(n) U^H(n) P(n-1)\right] U(n) \quad (4.27)$$

The equation in the bracket was same as Equation 4.25. Which means we can derive Equation 4.28.

$$K(n) = P(n) U(n) \quad (4.28)$$

Next, we need to obtain equation used to Update the tap weight vector least squares estimation. From the Equation 4.14. Equation 4.19. Equation 4.24. we can derive Equation 4.29.

$$\hat{W}(n) = \Phi^{-1}(n) Z(n) = P(n) Z(n) = \lambda P(n) Z(n-1) + P(n) U(n) d^*(n) \quad (4.29)$$

Use Equation 4.25. to replace most right $P(n)$ will get Equation 4.30.

$$\begin{aligned} \hat{W}(n) &= P(n-1) Z(n-1) - K(n) U^H(n) P(n-1) Z(n-1) + P(n) U(n) d^*(n) \\ &= \Phi^{-1}(n-1) Z(n-1) - K(n) U^H(n) \Phi^{-1}(n-1) Z(n-1) + P(n) U(n) d^*(n) \\ &= \hat{W}(n-1) - K(n) U^H(n) \hat{W}(n-1) + P(n) U(n) d^*(n) \end{aligned} \quad (4.30)$$

Because $P(n)U(n)$ equal to $K(n)$ .Equation 4.30. same as Equation 4.31.

$$\hat{W}(n) = \hat{W}(n-1) + K(n)\left[d^*(n) - U^H(n) \hat{W}(n-1)\right] = \hat{W}(n-1) + K(n) \xi^*(n) \quad (4.31)$$

In here

$$\xi(n) = d(n) - U^T(n) \hat{W}^*(n-1) = d(n) - \hat{W}^H(n-1) U(n) \quad (4.32)$$

Was a prior error, inner product $\hat{W}^H(n-1)U(n)$ express expectation response's value $d(n)$'s estimate value based on the previous value from Tap weight vector.

With all the Equation above, we can make a small summary here. At the start time. We have Equation 4.33.

$$\begin{aligned} W(0) &= 0 \\ P(0) &= \sigma^{-1} I \end{aligned} \quad (4.33)$$

For every iteration, we need to calculate Equation 4.34-4.37.

$$K(n) = \frac{P(n-1)U(n)}{\lambda + U^H(n)P(n-1)U(n)} \tag{4.34}$$

$$\xi(n) = d(n) - \hat{W}^H(n-1)U(n) \tag{4.35}$$

$$\hat{W}(n) = \hat{W}(n-1) + K(n)\xi^*(n) \tag{4.36}$$

$$P(n) = \lambda^{-1}P(n-1) - \lambda^{-1}K(n)U^H(n)P(n-1) \tag{4.37}$$

Here will be all the equations we need in the RLS algorithm. $K(n)$ is gain vector, ζ here are errors from previous estimate, Equation.4.36 means best filter at this moment, It update from old best filter and multiple by gain vector plus error, Equation 4.37 means updating inverse matrix which we obtain from matrix inversion lemma.

4.5 Summary

We still use RLS here to process the original data but with some little change, the change is that we always update the prediction model with time but only change the prediction model after the error surpasses a specific value. Which means we continue to use the previous prediction model and carry a current prediction with us, after error surpasses a specific value, we change the previous model to current model, and carry a new current model and continue to update it. By this particular method, we will be able to use the information from the camera to enhance the accuracy of the systems.

After all of those appropriate process, finally, we can get the result as Figure 4.4: The results of the sensor's output and prediction.. The horizontal axis was the time and the vertical axis was the object's degree compare to the horizontal line.

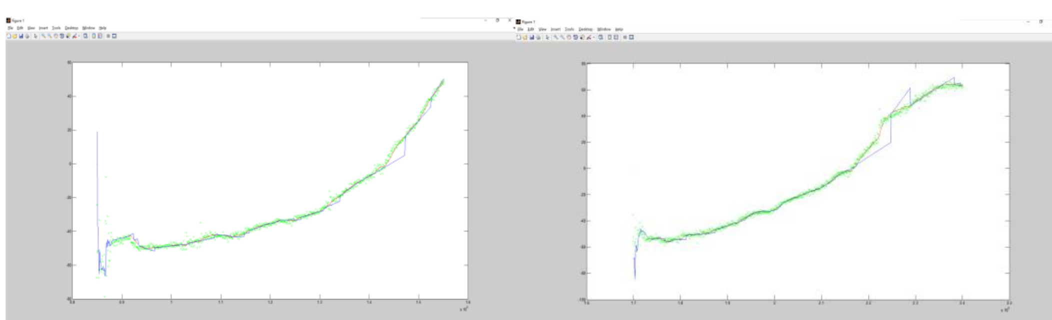

Figure 4.4: The results of the sensor's output and prediction.

The green mark was the original data without any process, read line is the original fit, we can only regression the red line after the all process use all data to do the linear regression, so, red line doesn't mean too much. Blue line here was the prediction data we got from the Recursive least square method in real time. It's obvious that the prediction line has some delay but reduce the noise significantly, those delay came from the previous prediction model because we keep using the previous prediction model before the error surpass a specific value, so, if the object's motion change but we didn't change the prediction model, the delay will occur, after the error gets too large, the prediction model has been replaced and the prediction line catch up the real line. Also, the original data sometimes has an obvious shift which can cause observe error. Those shifts usually were because the human's different habitual action, we have to admit that human has some random moving and those moving always didn't have any specific meaning but will bring the difficult for monitoring the torch's motion and velocity.

CHAPTER 5. **CONCLUSIONS AND FUTURE WORK**

5.1 Conclusion

Manual welding processes are still widely used in many manufacturing areas these days, such as car repair or shipbuilding industries. But the problem is that welding is also a skill-required operation which means a well-trained worker is very valuable and very lack. Since the difference between a new worker and an experienced worker is that how to control the process under different circumstance and how to determine what is going on during the welding process. Here the task of this thesis is try to provide a method that uses two different sensor’s compensate each other to get accurate monitoring result, the vision sensor’s calibration and real-time image processing, segmentation and track has been finished in CHAPTER 3 and the inertial measurement unit sensor’s calibration coordinate system set-up, mathematic model and prediction has been finished in CHAPTER 4.

5.2 Future work

The method in this thesis still can be improved by the next generation’s intelligent technology like machine learning. To make this method more practical and can be used. More future work can be done to improve the design of this method.

For the first improve, it is possible to build a Markov chain or decision tree to determined how to select data from these two sensors and how to use vision data to enhance the prediction model in the Recursive least square method.

Next Improve is to reduce the image processing algorithm’s time complex and space complex in order to build the system in a single-chip microcomputer, which means the monitoring process will be more easy to apply in a real working environment.

Furthermore, human welder’s behaviour can be modeling and considered as an adjusting parameter to develop human welder response model. Practically, a skilled welder may adjust torch orientation, speed or arc length during the process. A complex model is required in order to study human behavior during the welding process.

REFERENCES

[1] Zhang, WeiJie, "Machine-human Cooperative Control of Welding Process" (2014). *Theses and Dissertations--Electrical and Computer Engineering*. 45.

[2] Joint tracking robot system transforms companys welding production. *Welding Journal,* 73(3):68-69, 1994.

[3] B. Butler. Joint tracking automation triples propane cylinder production. *Welding Journal,* 71(8):61-63, 1992.

[4] R.B. Madigan. Ways to keep torches in seams. *Welding Design and Fabrication,* pages 48-50, 1987.

[5] Michael Jones. Robust Real-time Face Detection. *International Journal of Computer Vision,* 57(2):137-154, 2004.

[6] Ben-Hur A, Elisseeff A, Guyon I. A stability based method for discovering structure in clustered data. *Biocomputing,* 2002:6-17, 2002.

[7] Duarte M F, Eldar Y C. Structured Compressed Sensing: From Theory to Applications. *IEEE press,* 2011.

[8] J.R. QUINLAN. Induction of Decision Trees. *Machine Learning 1: 81-106,* 1986.

[9] Christian Forster, Luca Carlone, Frank Dellaert, and Davide Scaramuzza. IMU pre-integration on Manifold for Efficient Visual-Inertial Maximum-a-Posteriori Estimation. *Robotics: Science and Systems 2015, Rome, Italy, July* 13-17, 2015.

[10] Jared B. Bancroft, Gerard Lachapelle. Data Fusion Algorithms for Multiple Inertial Measurement Units. *Sensors, 2011, 11(7), 6771-6798; doi:10.3390/s110-706771.*

[11] Janne Heikkil and Olli Silvn. A four-step camera calibration procedure with implicit image correction. In *Proceedings of IEEE Computer Society Conference on -Computer Vision and Pattern Recognition,* 1997.

[12] Duane C. Brown. Close-range camera calibration. *PHOTOGRAMMETRIC ENGINE-ERING,* 37:855-866, 1971.

[13] J.G. Fryer and D.C. Brown. Lens distortion for close-range photogrammetry. *Photogrammetric Engineering and Remote Sensing,* 52:51-58, 1986.

[14] Peter F. Strum and Stephen J. Maybank. On plane-based camera calibration: a general algorithm, singularities, applications. In IEEE Computer Society Conference on Computer Vision and Pattern Recognition, 1999.

[15] Zhengyou Zhang. Flexible camera calibration by viewing a plane from unknow-orientation. *In the Proceedings of the 7th IEEE International Conference on Computer Vision,* 1999.

[16] Zhengyou Zhang. A flexible new technique for camera calibration. *In IEEE Transactions on Pattern Analysis and Machine Intelligence, volume 22, pages 13301-34,* 2000.

[17] Narayanan Ramakrishnan, Harish, "Detection and estimation of image blur" (2010). Masters Theses. 4804.

[18] Butler, S. (2008). Eigenvalues and structures of graphs. *UC San Diego*. ProQuest ID: umi-ucsd-2052.

[19] Baldev Raj, T. Jayakumar, and M. Thavasimuthu. *Practical non-destructive testing.* Woodhead Publishing, 2002.

[20] Hoobasar Rampaul. *Pipe welding procedures (2nd ed)* Industrial press, 2003.

[21] Klas Weman. *Welding processes handbook.* New York, NY: CRC Press,, 2003.

[22] J.C.K Chou. Quaternion kinematic and dynamic differential equations. *IEEE Transactions on Robotics and Automation,* 8(1):53-64, 1992.

[23] Giorgio De Pasquale and Aurelio Soma. Reliability testing procedure for mems imus applied to vibrating environments. Sensor, 10:456-474, 2010.

[24] Kian Sek Tee, Mohammed Awad, Abbas Dehghani, David Moser, and Saeed Zahedi, editors. Triaxial Accelerometer Static Calibration, *Proceedings of the World Congress on Engineering*, volume III, London, UK, July 2011.

[25] F. Ferraris, U. Grimaldi, and M. Pavis. Procedure for effortless in-field. Calibration of three-axis rate gyros and accelerometers. *Sensors and Materials*, 7:311:33-0,1995.

[26] IMU and NIMU temperature dependent bias, scale factor and cross sensitivity correction performance revision 1. Technical report, MEMSense.

VITA

Rui Yu was born in Xi’an, Shaanxi, China.

EDUCATION:

Xi’an University of Posts and Telecommunications, China 07/2014

B.S in information Engineering